Supplementary

High-Iodine-Loading Quasi-Solid-State Zinc-Iodine Batteries Enabled by a Continuous Ion-Transport Network

Xin Yang[a#], Minghao Xie[a#], Zhijie Yan[b], Hang Ruan[a], Chunpeng Yang*[b], Zaiping Guo*[c], Zi-Jian Zheng*[a]

Experimental section

Chemicals. Bacterial cellulose (BC) was purchased from Guilin Qihong Technology Co. Zinc sulfate heptahydrate ($ZnSO_4 \cdot 7H_2O$) and iodine monomers were purchased from Sinopharm Chemical Reagent Co. Zn foil was purchased from Saibo Electrochemical Materials Co. Polytetrafluoroethylene (PTFE) slurry (60%) and activated carbon were purchased from KELUDE Innovative Technology Co.

Preparation of iodine cathode materials. BC-based iodine cathode (BIC): self-supported activated carbon carriers were prepared by blending activated carbon (AC), BC, and conductive carbon in a weight ratio of 8:1:1 with deionized water as solvent. The obtained slurry was first placed in a container at 25 °C for natural drying, and then put into a vacuum oven at 80 °C for 12 h for fully drying. The BC-based iodine cathode was prepared by putting the prepared self-supported activated carbon carrier and iodine monomer with desired together into an autoclave then heat treated at 80 °C for 48 h. PTFE-based iodine cathode (PIC): Activated carbon, conductive carbon black and binder (PTFE) were put into an agate mortar in the weight ratio of 8:1:1, and appropriate amount of isopropyl alcohol was added and stirred thoroughly until the natural evaporation of isopropyl alcohol. The mixture was stirred until it turned into the state like plasticine. The compound was compacted into the stainless-steel mesh using roller pressing, followed by heat treatment in a vacuum oven at 80 °C for 12 h to ensure the complete removal of any residual isopropyl alcohol. The PTFE-based iodine cathode was prepared by combining the prepared carrier and iodine monomer in an autoclave, which was then heat-treated at 80 °C for 48 h.

Preparation of BC hydrogel electrolyte. The commercial bacterial cellulose hydrogels were immersed in a 4 wt.% NaOH aqueous solution for 6 h at room temperature, followed by thorough rinsing. Subsequently, the treated bacterial cellulose hydrogels were subjected to steaming at 90 °C for 3 hours and then washed with deionized water to ensure purification. The purified bacterial cellulose hydrogels were evenly placed in an appropriate container and first frozen in a refrigerator, followed by freeze drying in a freeze dryer to produce bacterial cellulose membranes. These membranes were then cut into discs with a diameter of 16 mm and immersed in a 2 M $ZnSO_4$ aqueous solution to prepare the bacterial cellulose-based hydrogel electrolyte.

Structural characterization

Surface morphology of the samples was characterized using a field emission scanning electron microscope (FE-SEM) (SIGMA500, Zeiss), equipped with an energy dispersive spectrometer (EDS) attachment (Bruker). The X-ray diffraction (XRD) patterns were recorded via Bruker-AXS micro-diffractometer (D8 ADVANCE) with Cu (Kα-rays, λ = 1.54 Å) at a current of 40 mA and a voltage of 40 kV was adopted to characterize the structure of the samples. Raman spectra was measured on Raman microscope (inVia, Renishao) with a Raman excitation wavelength of 532 nm and the power of 100%. In-situ UV-vis spectral was measured on UV-Vis spectrophotometers (UV-3600). The stress-strain test was performed on an Instron 68TM-10 (USA) universal tensile testing machine. X-ray photoelectron spectroscopy (XPS) test was measured on ESCALAB 250Xi (Thermo Fisher Scientific).

Electrochemical Measurements

The CR2025 type coin cells were assembled using BC-based hydrogel electrolyte or liquid electrolyte with glass fiber (GF) as separator, which were tested on a NEWARE battery test system. Electrochemical impedance spectroscopy (EIS) was recorded on the electrochemical workstation (PGSTAT302N, AutoLab) with a frequency range from 10 MHz to 0.1 Hz. Cyclic voltammetry (CV) was measured on the electrochemical workstation at a scanning speed of 1 mV s^{-1}. The DRT image is obtained by the DRTtools plug-in in Matlab. Linear sweep voltammetry (LSV) was measured on the

electrochemical workstation at a scanning speed of 5 mV s^{-1}. The ionic conductivity is calculated by the following formula: $\sigma = d/(R \cdot S)$, Where R represents the resistance measured according to EIS, d represents the thickness of the BC hydrogel electrolyte, and S is the contact area between the stainless-steel sheet and the electrolyte. The Coulombic efficiency is defined to be a ratio of the discharge capacities versus the charge capacities.

DFT calculations. All DFT calculations were carried out with Gaussian 16 program. Structure optimization of the all models was conducted by B3LYP-D3(BJ)/def2-SVP to guarantee the simulated models at an optimized structure. The electrostatic potential (ESP) maps and molecular dipole moment (μ) were obtained through a single point energy calculation on the refined structure. The binding energy between BC or PTFE and iodine species was obtained at B3LYP/def2-TZVP level.

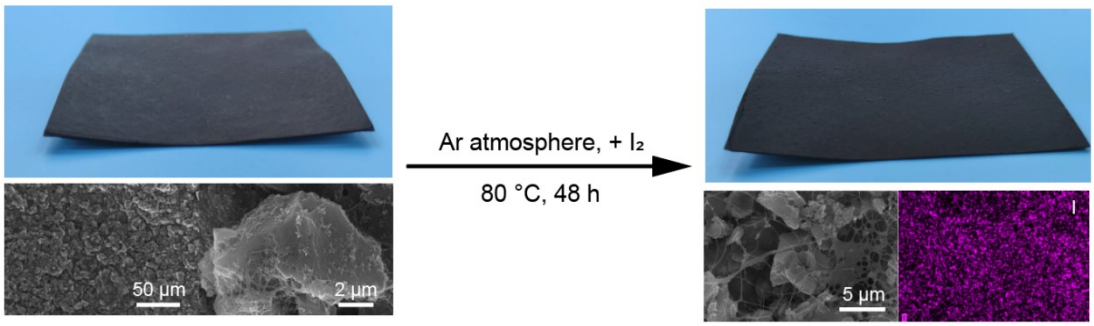

Figure S1. Production process of BC-based iodine cathode (BIC).

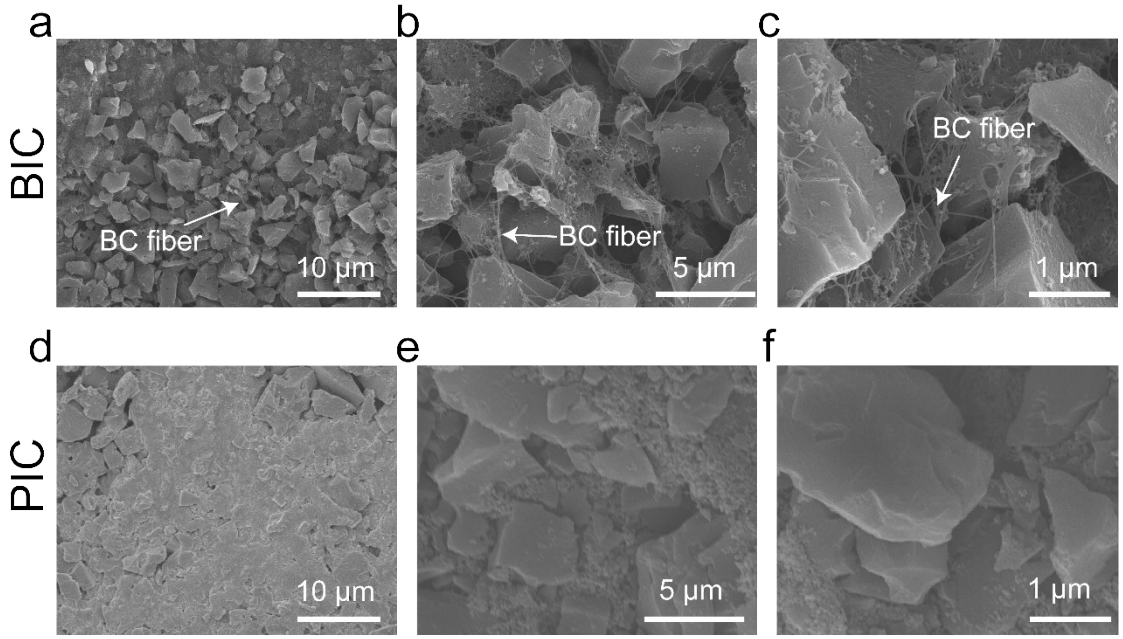

Figure S2. (a-c) SEM images of BIC and (d-f) PIC with increasing magnifications.

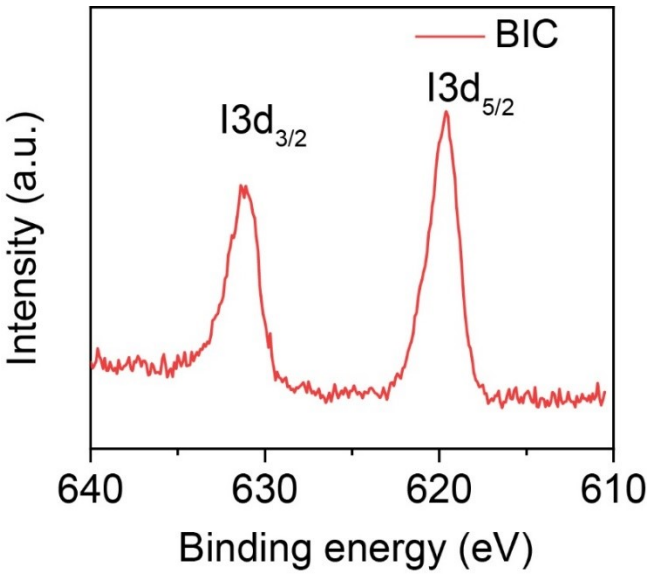

Figure S3. XPS curve of BIC.

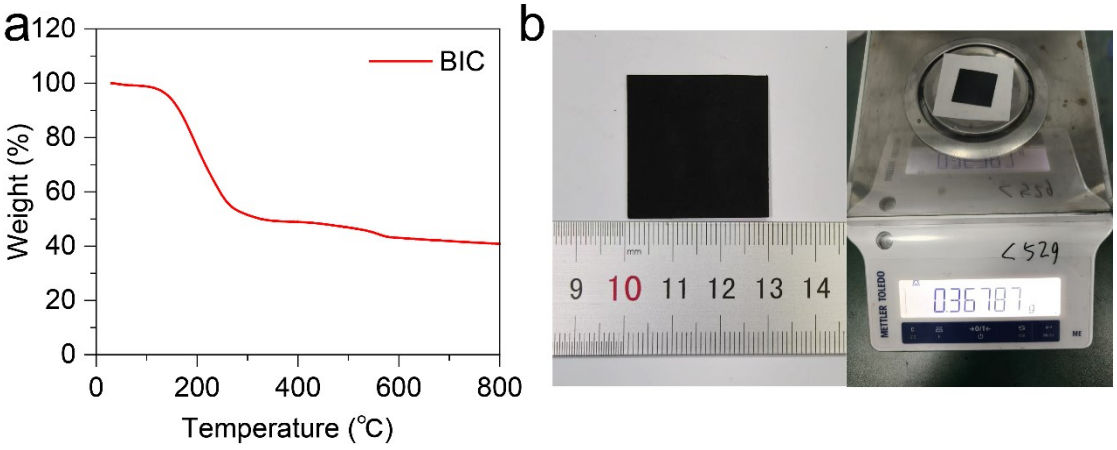

Figure S4. (a) TG test of BIC after iodine loading. (b) Optical photograph of the BIC and the quality of BIC (3 cm x 3 cm) after iodine loading.

To qualitatively assess the active iodine content in the BIC, we performed thermalgravimetric analysis (TGA) under a N_2 atmosphere. The results indicated significant weight loss beginning at approximately 300 °C, a temperature associated with the sublimation of iodine. The mass of I_2 accounts for about 49% of the total mass. For example, for a BIC sample with an iodide loading of 20 mg cm^{-2}, the calculations are as follows: the total mass of a BIC sample (3 cm x 3 cm) was measured to be 367.87 mg. The iodine loading in the BIC is estimated using the formula: 367.87 mg × 49% ÷ 9 cm^2.

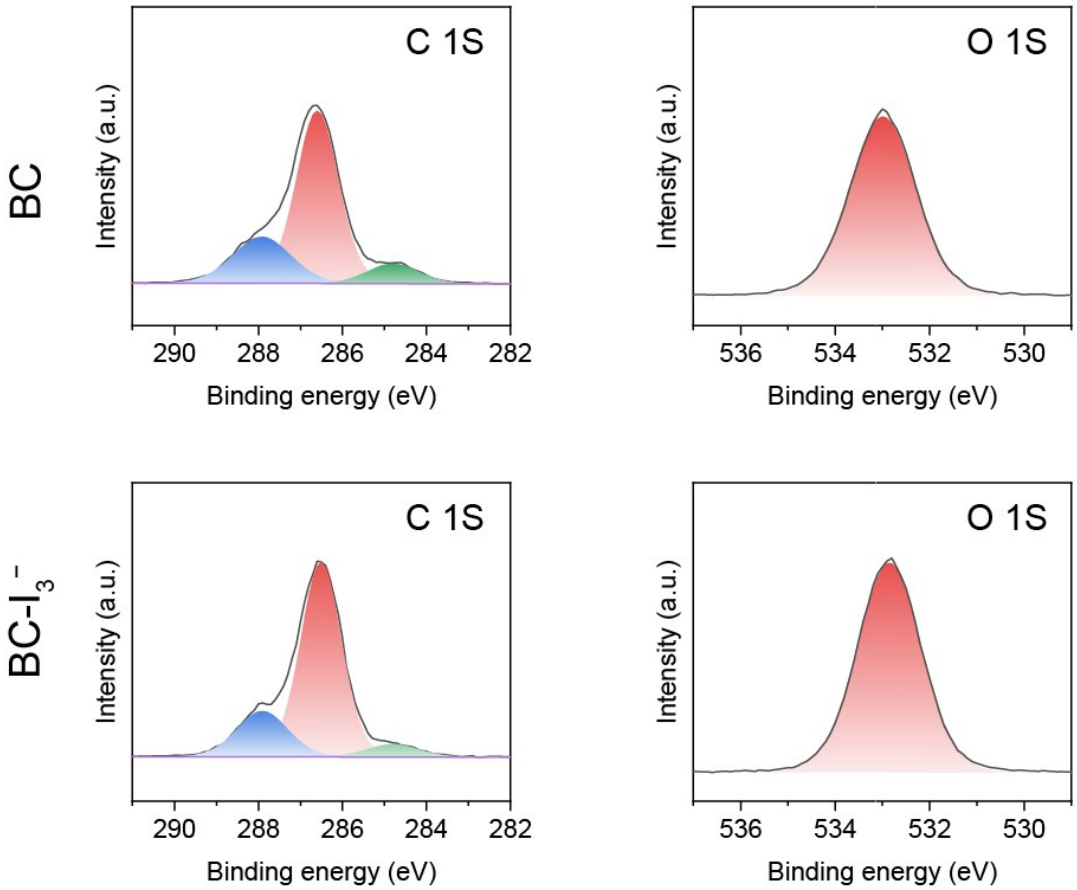

Figure S5. C 1s, O 1s XPS patterns of BC and BC@I_3^-.

Figure S6. A digital photo of a 30 cm × 25 cm BC hydrogel membrane.

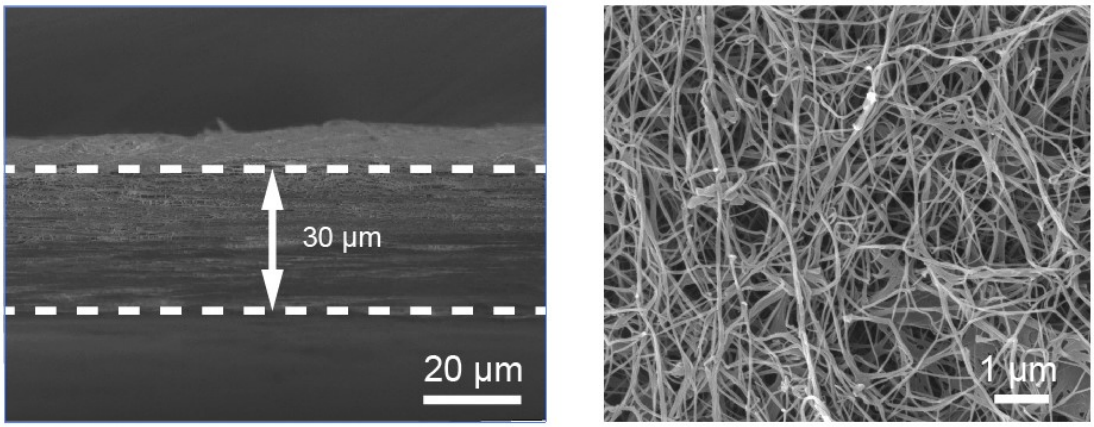

Figure S7. SEM image of cross-section (left) and microstructure (right) of a dry BC membrane.

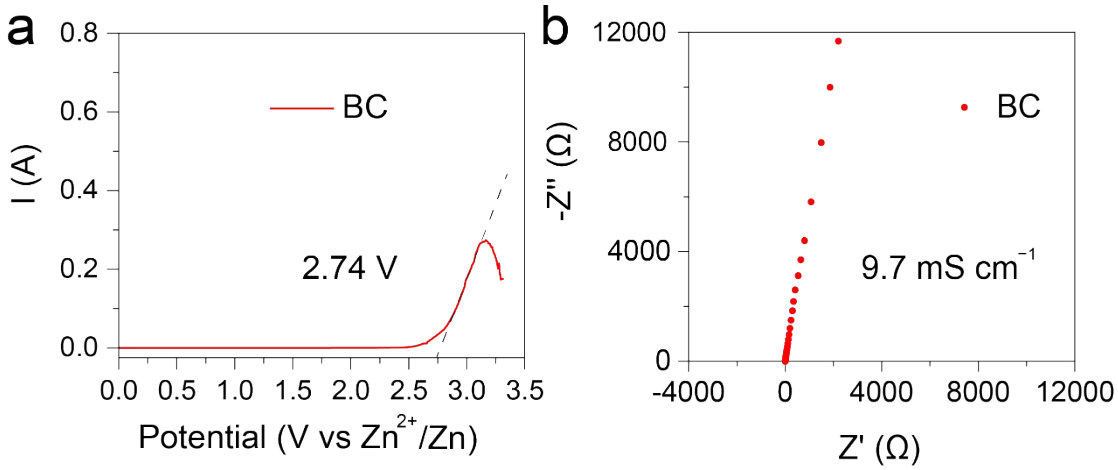

Figure S8. (a) Linear sweep voltammetry (LSV) test of BC hydrogel electrolyte. (b) Ionic conductivity of BC hydrogel electrolyte.

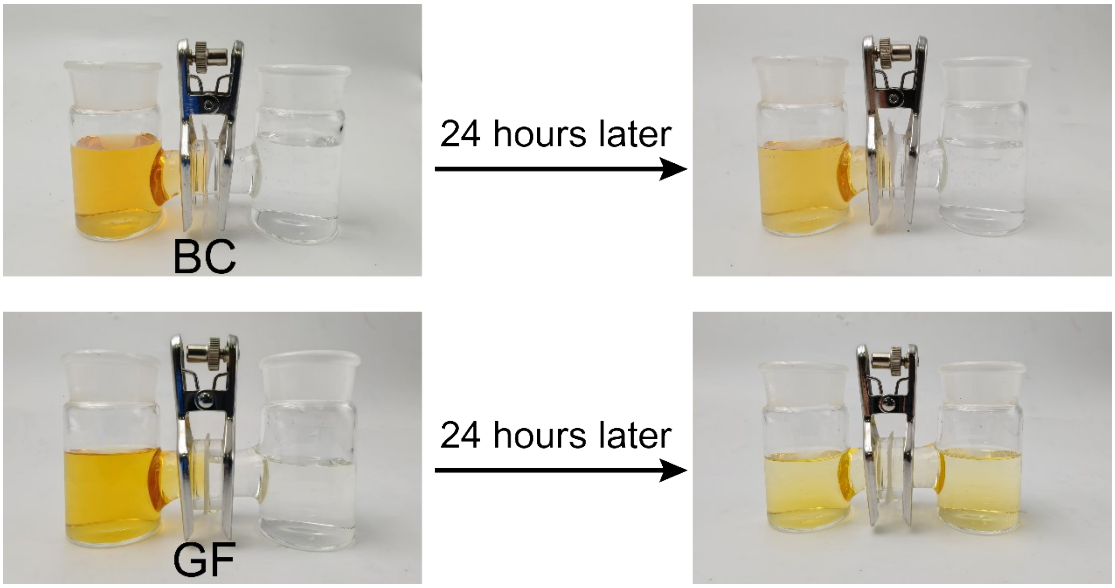

Figure S9. Optical photograph of BC membrane/GF separator separates a saturated iodine solution from a $ZnSO_4$ solution.

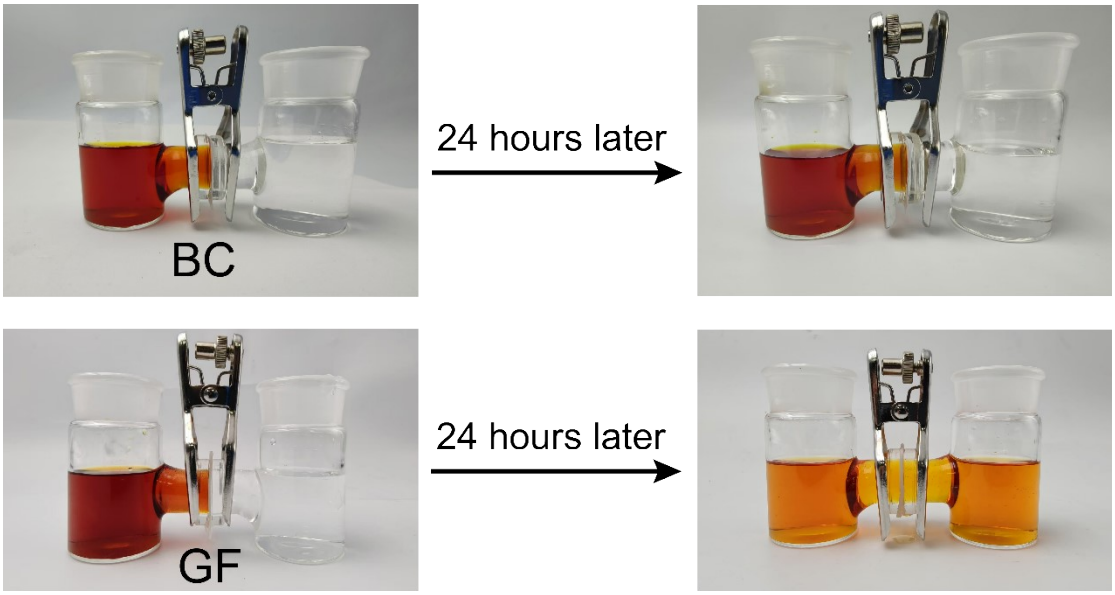

Figure S10. Optical photograph of BC membrane/GF separator separates a polyiodide solution from a $ZnSO_4$ solution.

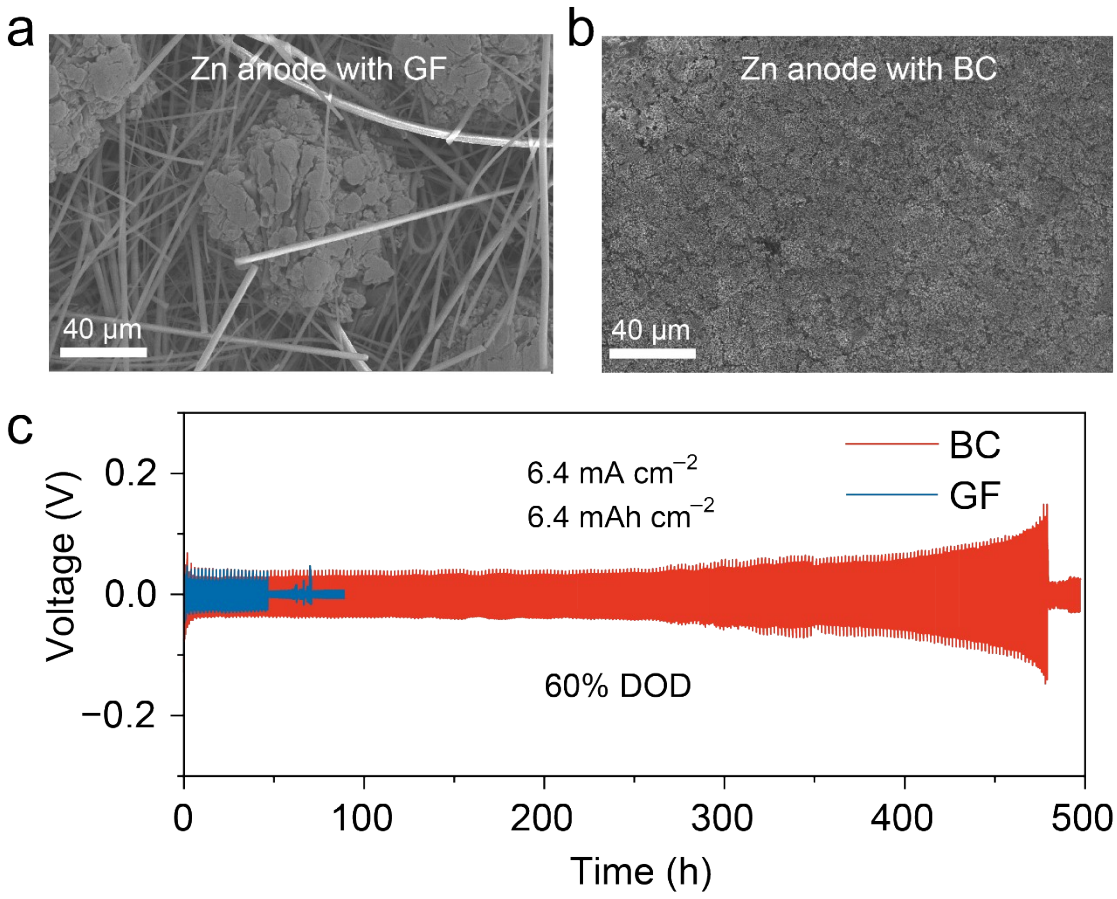

Figure S11. SEM images of the Zn anode after cycling for 50 h with (a) GF separator and (b) BC hydrogel electrolyte at 6.4 mA cm^{-2} and 6.4 m Ah cm^{-2}. (c) Zn||Zn cells cycle at 60% DOD.

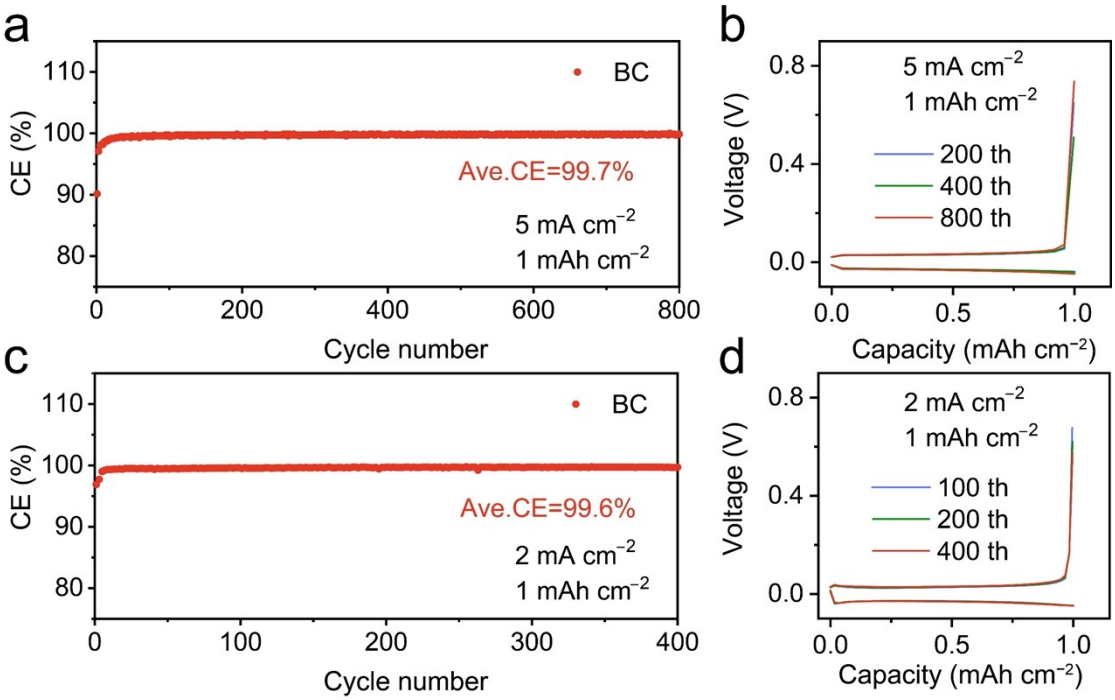

Figure S12. Coulombic efficiency (CE) measurements of Zn||Cu asymmetric cells at (a,b) 5 mA cm^{-2}, 1 mAh cm^{-2} and (c,d) 2 mA cm^{-2}, 1 mAh cm^{-2}.

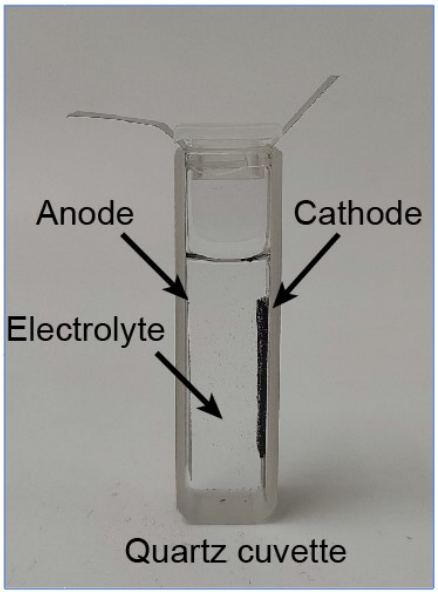

Figure S13. Apparatus for in situ UV testing of iodine dissolution. A simple zinc-iodine battery based on BIC or PIC, Zn anode, and 2 mL liquid electrolyte (2 M $ZnSO_4$) was assembled to assess the polyiodide dissolution behavior from the cathode to the electrolyte during the discharge process.

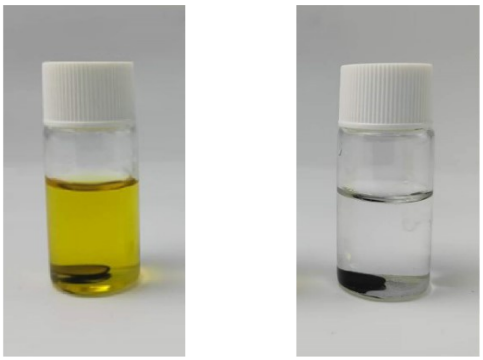

Figure S14. Optical photograph of the PIC and BIC cathodes after immersion in the water for 30 days.

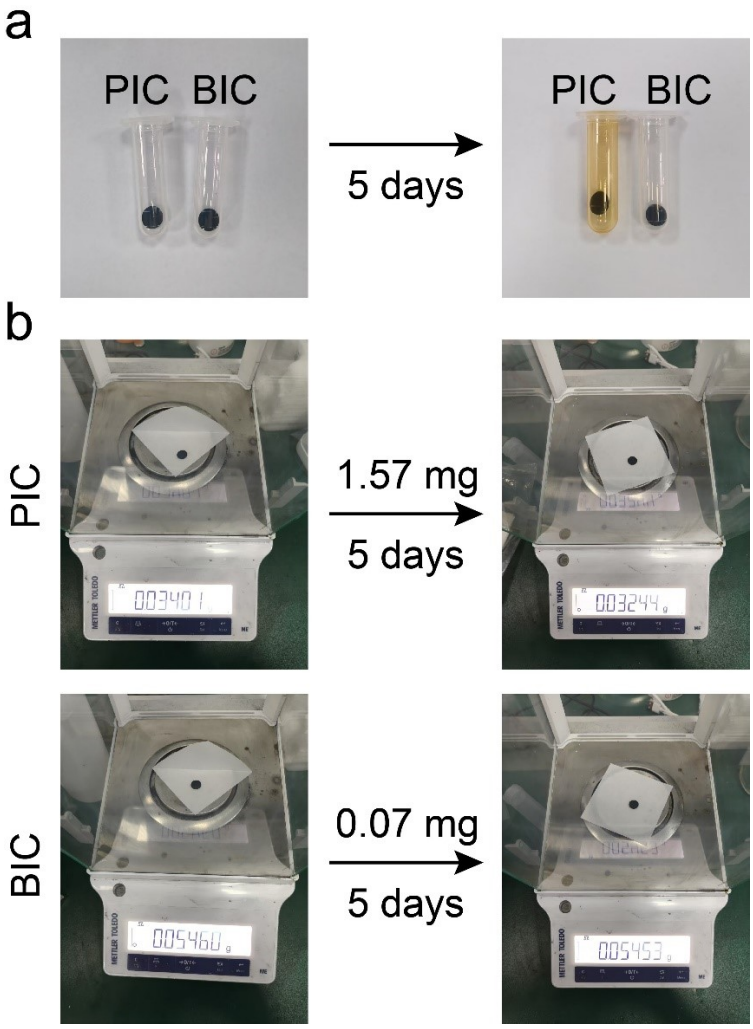

Figure S15. (a) Comparison of the resting stability between BIC and PIC. (b) Mass variation of BIC and PIC after 5 days of ambient storage.

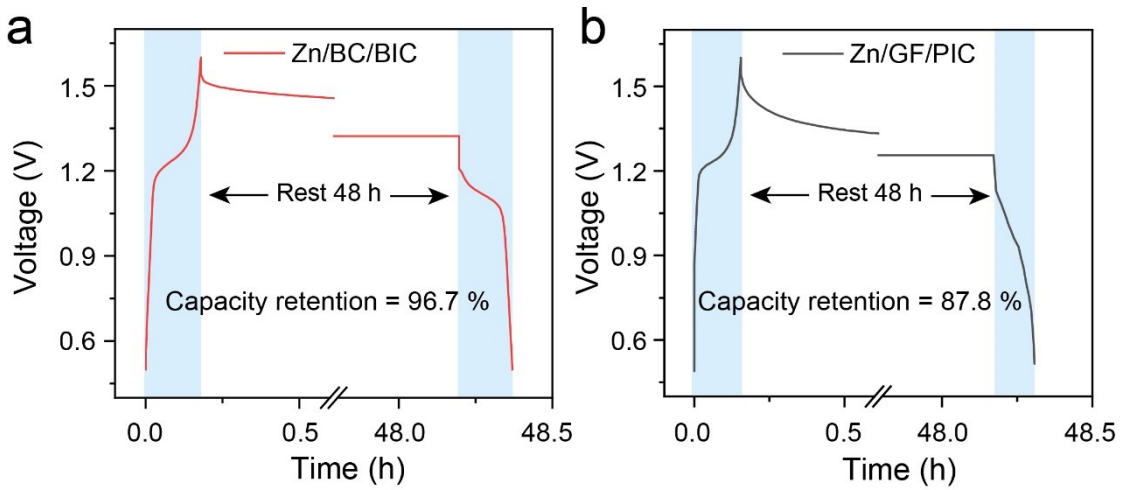

Figure S16. (a) Self-discharge test of Zn/BC/BIC. (b) Self-discharge test of Zn/GF/PIC.

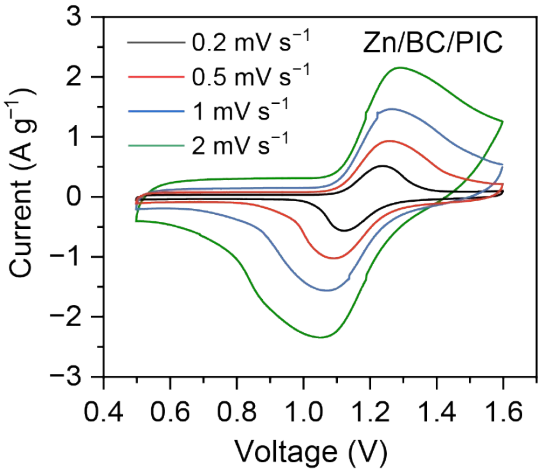

Figure S17. CV curves of Zn/BC/PIC.

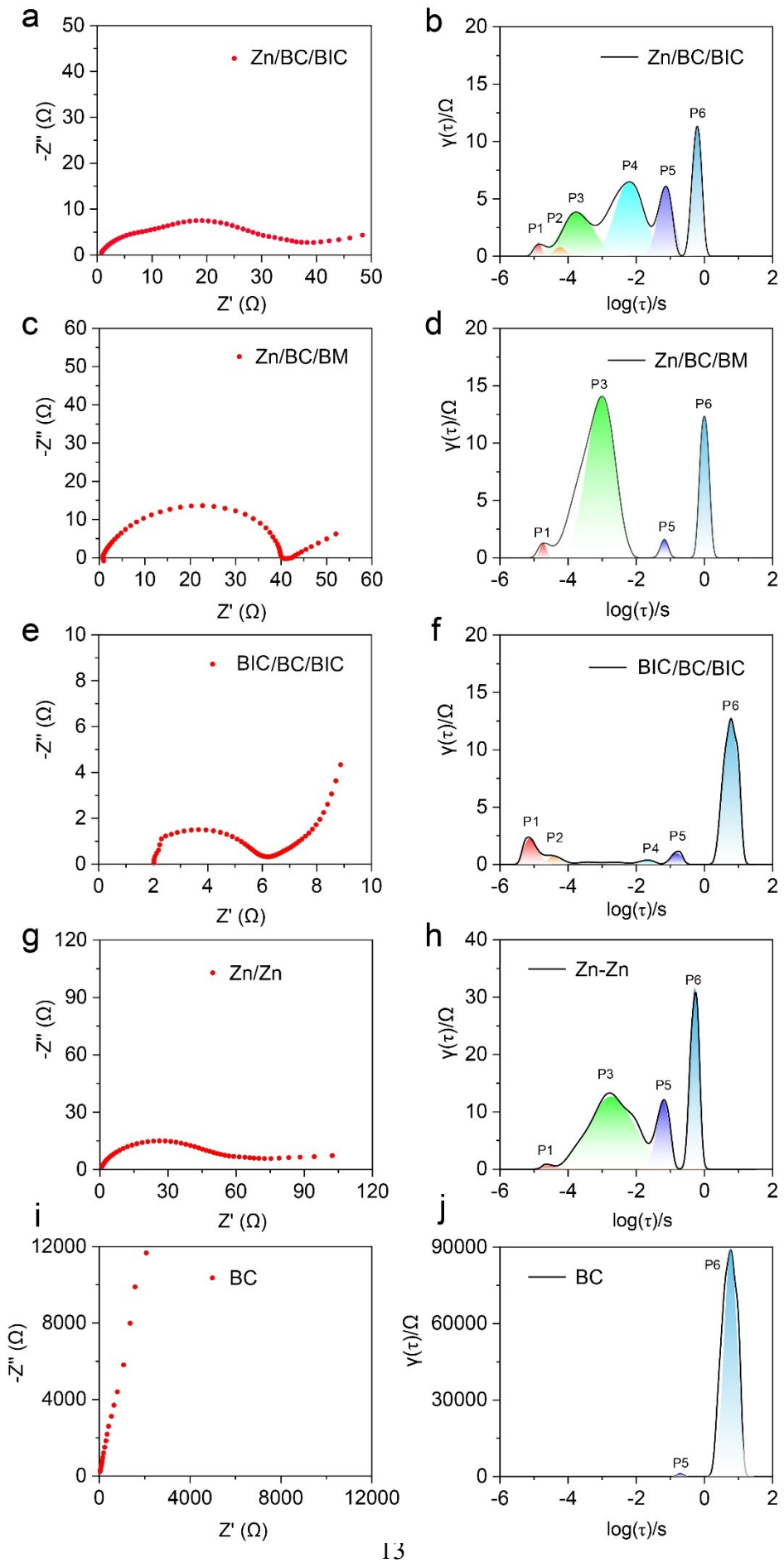
a
Zn/BC/BIC
-Z'' (Ω)
Z' (Ω)
b
Zn/BC/BIC
γ(τ)/Ω
log(τ)/s
P1
P2
P3
P4
P5
P6
c
Zn/BC/BM
d
Zn/BC/BM
e
BIC/BC/BIC
f
BIC/BC/BIC
g
Zn/Zn
h
Zn-Zn
i
BC
j
BC

Figure S18. (a, b**)** EIS curve and DRT curve of Zn/BC/BIC; (c, d**)** EIS curve and DRT curve of Zn/BC/BM. Here BM denotes BC-based membrane, which is prepared by a mixture of activated carbon (AC), BC, and conductive carbon with a weight ratio of 8:1:1. (e, f**)** EIS curve and DRT curve of symmetric BIC/BC/BIC battery; (g, h) EIS curve and DRT curve of symmetric Zn/Zn battery; (i, j) EIS curve and DRT curve of only BC hydrogel electrolyte battery.

P1 (Figure S18b) shows rapid relaxation behavior, which can be assigned to the total Ohmic resistance originating from ionic/electronic resistance of the electrodes. P2 exists in both Zn/BC/BIC (Figure S18b) and BIC/BC/BIC (Figure S18f) system, which may be related to the relaxation of the double electric layer of the positive electrode. P3 exists in Zn/BC/BIC (Figure S18b), Zn/BC/BM (Figure S18d), and Zn/Zn (Figure S18h), but not exists in BIC/BC/BIC (Figure S18f), suggesting that this peak is associated with the interfacial migration of zinc ions. Compared to Zn/BC/BM (Figure S18b), there is P4 in Zn/BC/BIC (Figure S18d) and BIC/BC/BIC (Figure S18f) system, demonstrating that this peak is related to the charge transfer of the active substance of the positive electrode material. Only P5 and P6 were observed in the cell with the BC hydrogel electrolyte (Figure S18j), and these two peaks were also present in all batteries, which can be contributed to the ion diffusion behavior.

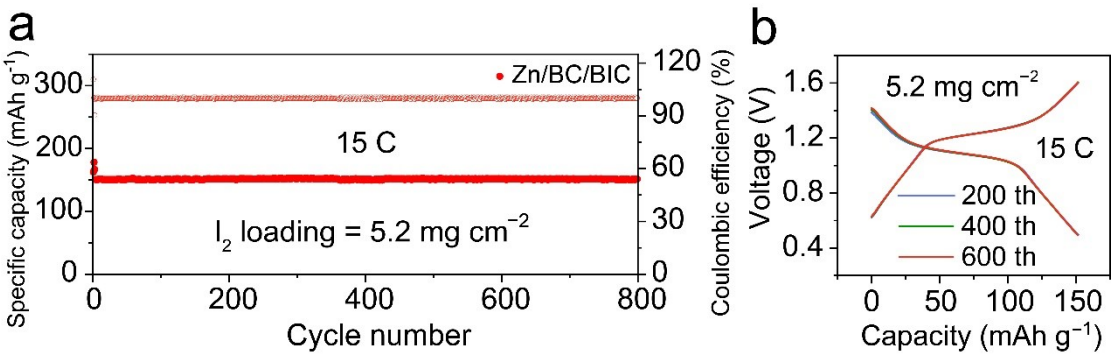

Figure S19. (a) Long-term cycling performance and (b) capacity-voltage curves of Zn/BC/BIC with a I_2 loading of 5.2 mg cm^{-2} at 15 C.

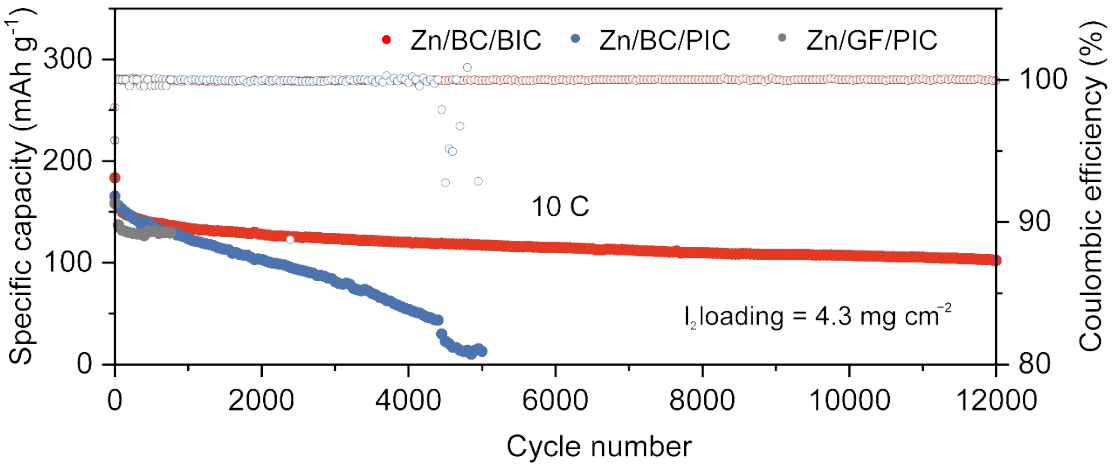

Figure S20. Long-term cycling performance of Zn/BC/BIC, Zn/BC/PIC, and Zn/GF/PIC with a I_2 loading of 4.3 mg cm^{-2} at 10 C.

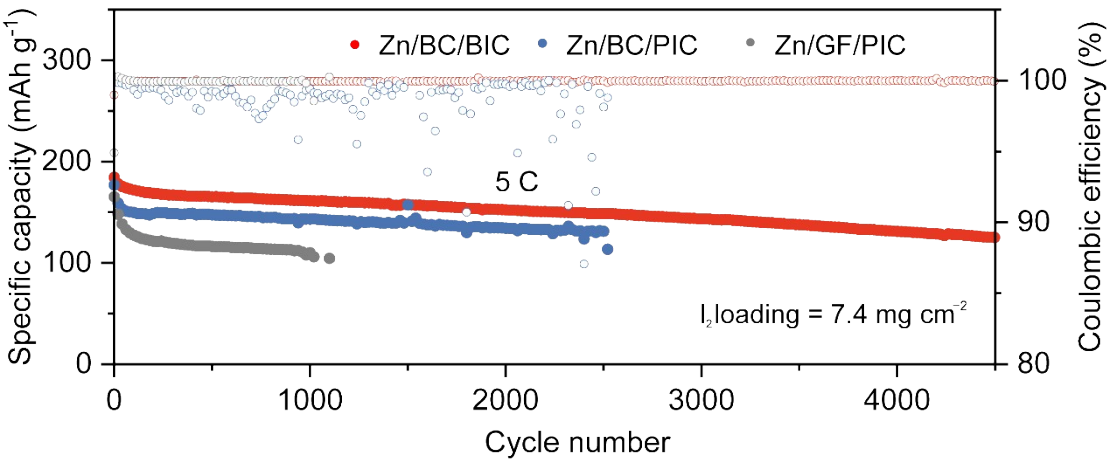

Figure S21. Long-term cycling performance of Zn/BC/BIC, Zn/BC/PIC, and Zn/GF/PIC with a I_2 loading of 7.4 mg cm^{-2} at 5 C.

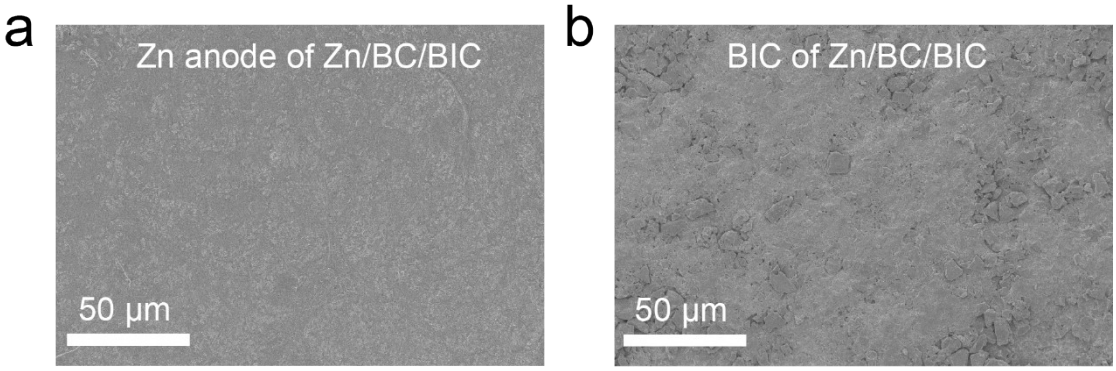

Figure S22. SEM images of (a) Zn anode and (b) BIC cathode of Zn/BC/BIC with a I_2 loading of 20.0 mg cm^{-2} after 100 cycles.

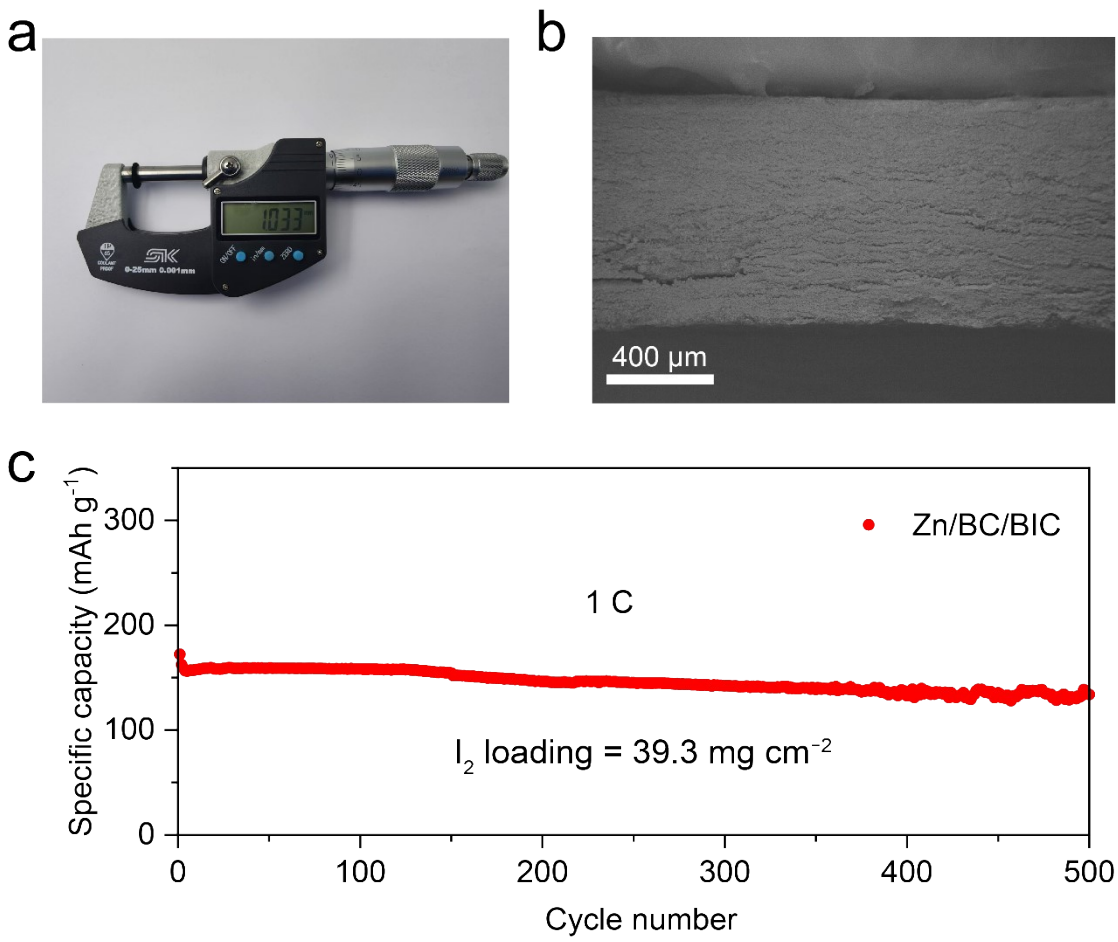

Figure S23. (a) optical photo and (b) cross-section SEM images of the designed thick BIC. (c) Long-term cycling performance of Zn/BC/BIC coin cell at 1 C with a I_2 loading of 39.3 mg cm^{-2}.

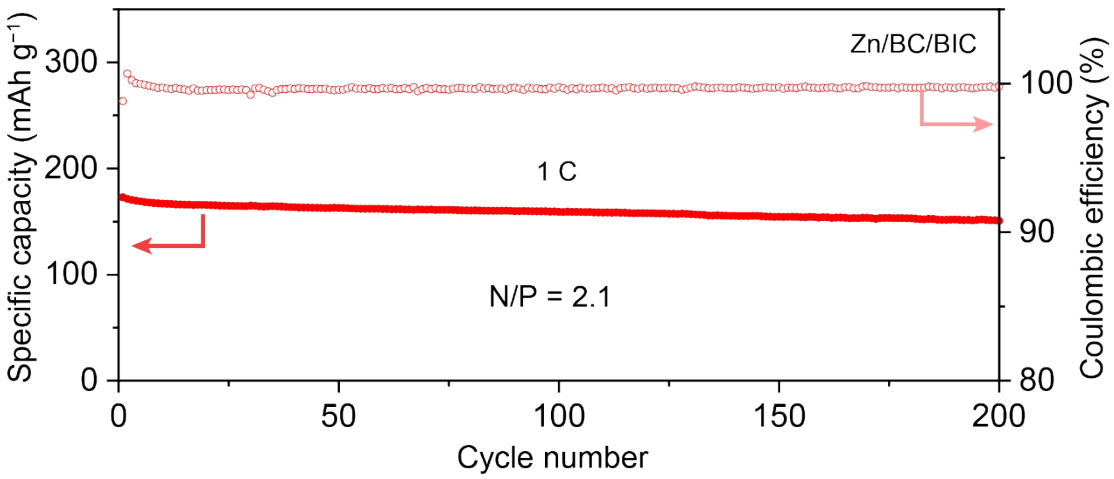

Figure S24. Long-term cycling performance of Zn/BC/BIC under the low N/P of 2.1 at 1 C.

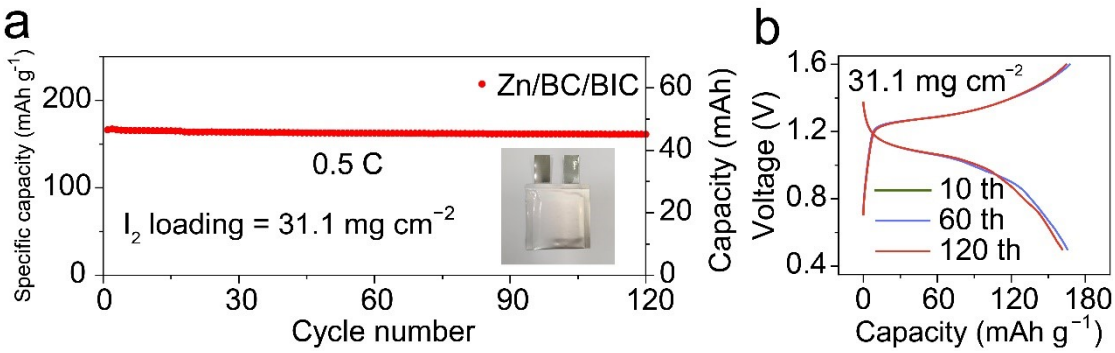

Figure S25. (a) Long-term cycling performance and (b) capacity-voltage curves (b) of Zn/BC/BIC pouch cell at I_2 loading of 31.1 mg cm^{-2} at 0.5 C.

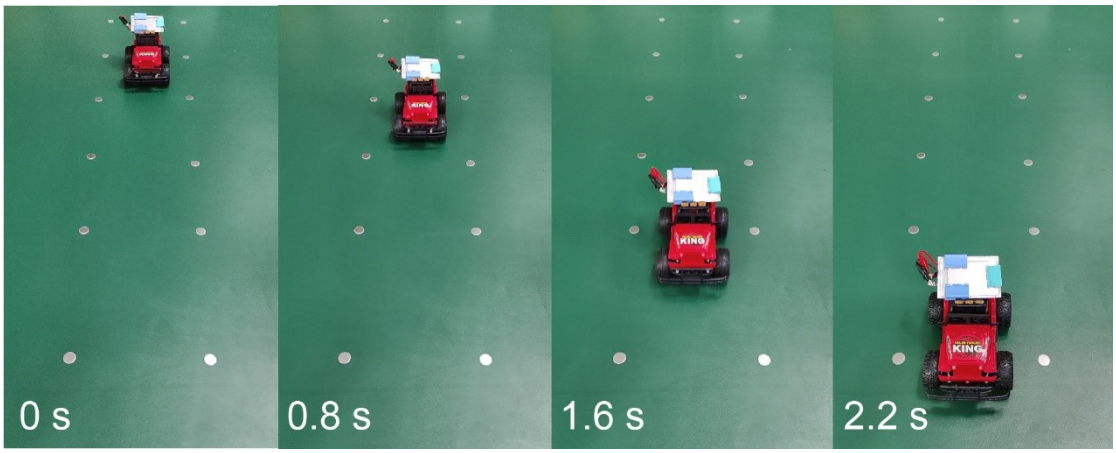

Figure S26. Digital images of a toy car driving by a pouch Zn/BC/BIC battery connected in series.

Table S1. The weight of the main components of the full Zn-I_2 battery and the calculated energy density of the full battery.

Battery component	Iodine	Total cathode	Zinc anode	BC hydrogel electrolyte	Energy density
Wight (mg)	16.5	33.2	9.2	15.7	56.4 Wh kg^{-1}

$$Energy\ density = C \times V \div M = 172.8\ mAh\ g^{-1} \times 16.5\ mg \times 1.15\ V \div 58.1\ mg = 56.4\ Wh\ kg^{-1}$$